

# Analytical Methods

Accepted Manuscript



This is an *Accepted Manuscript*, which has been through the Royal Society of Chemistry peer review process and has been accepted for publication.

*Accepted Manuscripts* are published online shortly after acceptance, before technical editing, formatting and proof reading. Using this free service, authors can make their results available to the community, in citable form, before we publish the edited article. We will replace this *Accepted Manuscript* with the edited and formatted *Advance Article* as soon as it is available.

You can find more information about *Accepted Manuscripts* in the [Information for Authors](#).

Please note that technical editing may introduce minor changes to the text and/or graphics, which may alter content. The journal's standard [Terms & Conditions](#) and the [Ethical guidelines](#) still apply. In no event shall the Royal Society of Chemistry be held responsible for any errors or omissions in this *Accepted Manuscript* or any consequences arising from the use of any information it contains.

## COMMUNICATION

# Studying the membrane structure of chicken erythrocytes by *in situ* atomic force microscopy

Cite this: DOI: 10.1039/x0xx00000x

Yongmei Tian<sup>a,b</sup>, Mingjun Cai<sup>b</sup>, Haijiao Xu<sup>b</sup>, and Hongda Wang<sup>\*,b</sup>Received 00th January 2014,  
Accepted 00th January 2014

DOI: 10.1039/x0xx00000x

[www.rsc.org/](http://www.rsc.org/)

**High resolution atomic force microscopy and single molecule force spectroscopy revealed the asymmetric distribution of proteins on both sides of chicken erythrocyte membranes. The cholesterol-enriched domains were directly observed by *in situ* atomic force microscopy, providing the first direct evidence of lipid rafts in chicken erythrocyte membranes.**

## Introduction

The cell membrane (plasma membranes) surrounds the cytoplasm of living cells, physically separating the intracellular components from the extracellular environment. The cell membrane serves as a dynamic platform for localization of various components including lipids, proteins, carbohydrates and so on, which actively participate in many aspects of cellular activities such as signal transduction, membrane transport and energy conversion<sup>1-4</sup>. The elaborate structure and organization of cell membranes is fundamental for cells to perform these complicated functions. The cell membrane structure, mainly distribution of lipids and proteins, has been extensively studied for decades<sup>5-7</sup>. Erythrocyte, as the simplest cell in living organism, was usually used as a model for the study of cell membrane structure. Recently, the semi-mosaic model has been introduced to illustrate the membrane structure of human<sup>8</sup> and fish<sup>9</sup> erythrocytes. It is of great significance to systematically study erythrocyte membrane structure following the evolution law. Chicken is one of the most common and widespread domestic fowl, whose phylogenetic position within Galliformes is near the base of Phasianidae<sup>10</sup>. There are more chickens in the world than any other species of birds. The study of chicken erythrocyte membrane structure, as a representative of birds, will bridge the gap between fish and mammalian.

The basic cytoarchitecture of erythrocytes has been largely conserved throughout the history of phylogenetic evolution, although it is possible that some variations in different species occurred<sup>11</sup>. Morphologically similar with fish erythrocytes,

chicken erythrocytes are nucleated, oval, biconvex discs, which is very different from non-nucleated, biconcave disc-like human erythrocytes<sup>12</sup>. As reported, chicken, fish and human erythrocyte membranes possess many features in common, including major membrane protein and phospholipid composition<sup>13-15</sup>. Whether or not the semi-mosaic model is adaptable to the membrane structure of chicken nucleated erythrocyte? How the chicken erythrocyte membranes are structured at the molecule level and where the membrane proteins are distributed? This study was undertaken with the aim of finding more about the similarities and differences in erythrocyte membrane structure of these species.

Atomic Force Microscopy (AFM) is well known as a multifunctional nanoscale tool in biological studies. With the advantage of imaging biological specimens under physiological conditions without the need for staining or fixation, AFM has been used to obtain high resolution topography of cell membranes<sup>8, 16</sup>, membrane proteins<sup>17</sup> and organelle<sup>18, 19</sup>. Recently, high speed AFM has created new opportunities for visualizing dynamic cellular events<sup>20, 21</sup>. The lipid rafts in model membrane had been observed by real-time AFM<sup>22</sup>. Our results have successfully confirmed the existence of lipid rafts in human erythrocytes membranes by *in-situ* and time-lapse AFM<sup>23</sup>. There are few reports on the surface features of chicken erythrocytes studied by AFM<sup>24</sup>. Herein, we utilized AFM to investigate the exquisite membrane structure of chicken erythrocytes, revealing the asymmetric distribution of proteins on the outer and inner leaflet of erythrocyte membranes.

## Results

### AFM imaging of the intact chicken erythrocytes and the outer leaflet of erythrocyte membranes

When imaged by AFM in physiological buffer solution, the isolated chicken erythrocytes firmly attached onto the substrate represent oval discs with elliptical nucleus highly protruding in

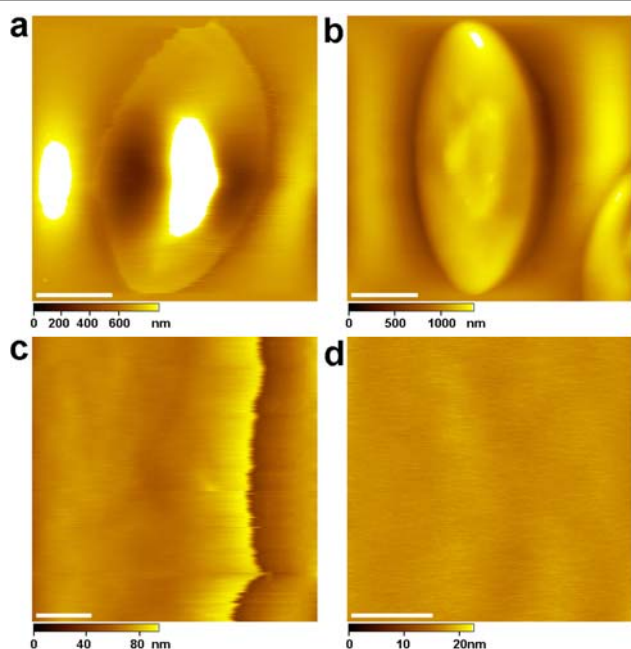


Fig. 1 Representative AFM topographic images of the intact chicken erythrocyte and the outer leaflet of erythrocyte membranes. (a) Unfixed chicken erythrocyte. (b) Chicken erythrocyte fixed by 4% paraformaldehyde. (c) The unfixed chicken erythrocyte appears quite smooth on the edge. (d) High resolution image shows no detectable protrusions or particles on the smooth outer surface. Scale bars: 5  $\mu\text{m}$  in (a) and (b), 500 nm in (c) and 200 nm in (d).

the central region (Fig.1a), which is similar with nucleated fish erythrocyte except the smaller size. The intact chicken erythrocyte is measured to be  $14.2 \pm 3.0 \mu\text{m}$  in long axis,  $8.9 \pm 1.6 \mu\text{m}$  in short axis and  $1.2 \pm 0.4 \mu\text{m}$  in height, while the nucleus has the length of  $6.8 \pm 1.9 \mu\text{m}$ , and width of  $4.3 \pm 0.7 \mu\text{m}$ . Without fixation, the outer surface of erythrocyte appears quite smooth in the edge. Fig.1b shows the topographical image of the intact fixed chicken erythrocyte, in which the oval erythrocyte appears fleshy in the edge as a result of fixation procedure. The intact fixed chicken erythrocyte is  $16.2 \pm 2.6 \mu\text{m}$  in long axis,  $8.9 \pm 1.0 \mu\text{m}$  in short axis and  $1.7 \pm 0.2 \mu\text{m}$  in height with elliptical nucleus  $8.7 \pm 1.2 \mu\text{m}$  long and  $5.0 \pm 0.6 \mu\text{m}$  wide. In both cases, the outer surface of erythrocyte is quite smooth in the edge. The intact unfixed chicken erythrocyte is measured to be  $45.6 \pm 1.4 \text{ nm}$  thick on the edge.

To observe more detailed features of the outer leaflet of erythrocyte membrane, we engaged high resolution imaging on the flattened edge of unfixed erythrocyte (Fig.1c). As expected, the outer surface of chicken erythrocytes is rather smooth with no obvious proteins or wrinkles. Higher resolution image was achieved, as seen in Fig.1d, which shows no detectable protrusions or particles on the smooth outer surface. The average roughness of the outer leaflet of chicken erythrocyte membranes was measured to be  $0.47 \pm 0.05 \text{ nm}$ , which demonstrates that the membrane surface is extremely smooth.

#### AFM imaging of the inner leaflets of erythrocyte membranes

The inner leaflets of chicken erythrocyte membranes, prepared by the shear-open method, display protein-decorated topography

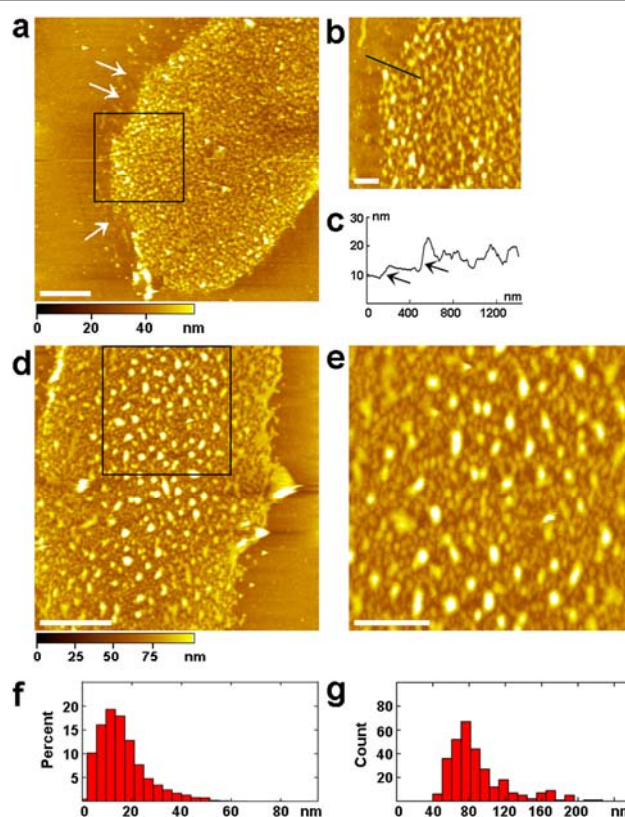


Fig. 2 AFM topographic image of the inner leaflet of chicken erythrocyte membranes. In (a), arrows point to the free lipid bilayers under the membrane proteins. (b) Magnification of the square area in (a). (c) Cross section analysis along the line in (b). Arrows point to free lipid bilayer and the protein layer, respectively. (d), (e) Median and high resolution image of the inner leaflet. (f), (g) The height and diameter distribution of proteins in the inner membrane leaflet, respectively. Scale bars: 2  $\mu\text{m}$  in (a) and (d), 500 nm in (b) and 1  $\mu\text{m}$  in (e).

(Fig.2a) after removal of membrane skeletons by high salt treatment. The shear-open method has previously been used to prepare the inner leaflet membranes of erythrocyte<sup>8, 23</sup>, demonstrated to be a good method to obtain clean membranes for high resolution AFM images and simultaneously keep the membrane structure intact. The prepared erythrocyte membranes show elliptical profile resembling that of intact erythrocytes, indicating that the upper surface membrane and cytoplasm components were totally sheared away. The height of the inner membrane leaflet was measured to be  $16.5 \pm 3.6 \text{ nm}$  between the substrate and the proteins. The average roughness of the inner membrane leaflet is about  $3.4 \pm 0.8 \text{ nm}$ , which is remarkably larger than that of the outer membrane. The arrows in Fig.2a point to free lipid bilayers on the edge of the membranes with the height of  $3.1 \pm 0.7 \text{ nm}$ , which is in complete accordance with the value measured by AFM<sup>8</sup>. Fig.2b is the magnified image of the square area in Fig.2A, which clearly shows the protein layer is just above the lipid bilayer. There are two clear steps shown by the cross section analysis in Fig. 2c in which the arrows point to the protein layer (right) and the free lipid bilayer (left), respectively.

Fig.2d is the middle resolution image of the inner leaflet of erythrocyte membranes, showing crowded protein particles with

no free lipid bilayer visible. Higher resolution image of the square area in Fig.2d was achieved. As seen in Fig.2e, the proteins are standing closely to each other and exhibit great variability in size and shape. As depicted in Fig.2f, the height of the protein particles above the membrane varies from 1.0 nm to 35.0 nm with the peak at 10 to 13 nm, corresponding to varieties of proteins and protein aggregations in the inner membrane leaflet, including Na<sup>+</sup>-K<sup>+</sup> pump, band 3 protein, glycophorin, etc<sup>15, 25, 26</sup>. These proteins display a broad diameter distribution from 45 nm to 250 nm with 75% in the range of 55 to 100 nm as shown in Fig.2g, which is a little larger than real protein particles due to the geometry of the cantilever tip<sup>27</sup> or protein aggregation.

### Digestion of the inner leaflets of erythrocyte membranes by Proteinase K

To further confirm the location of proteins above the lipid bilayer, we digested the inner membrane leaflet by Proteinase K. As shown in Fig.3a, most of the membrane proteins were digested after Proteinase K treatment, only separated peptides or proteins are visible just above the lipid bilayer. At the edge of the membranes, there are more free lipid bilayers (indicated by arrows) due to the lack of membrane proteins. The height of the lipid bilayer is  $3.8 \pm 0.5$  nm, which is consistent with that in Fig.2a. Fig.3b is the magnified image of the square area in Fig.3a with arrows pointing to small peptides remaining after Proteinase K digestion. Fig.3c shows the cross section along the line on the three peptides in Fig.3b. The height distribution of undigested proteins and peptides above the membrane ranges from 1.0 nm to 12.0 nm with the peak at 3 to 5 nm (Fig.3e), which is greatly lower than the untreated one (Fig.2f).

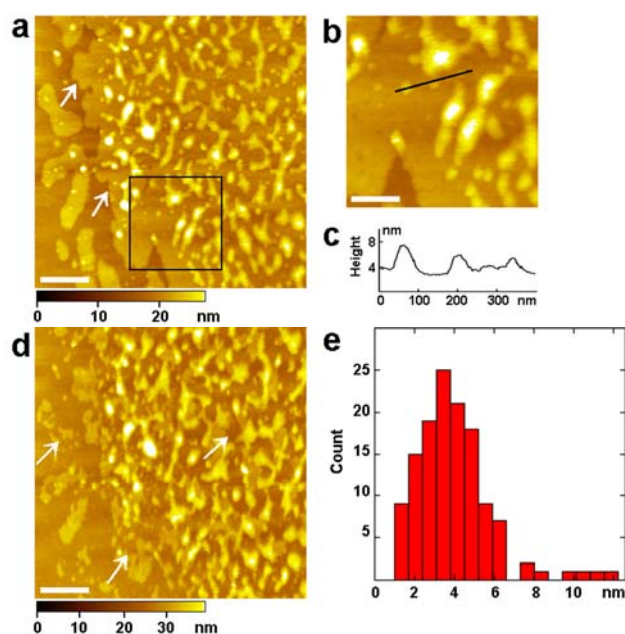


Fig. 3 AFM topographic image of the inner membrane leaflet digested by Proteinase K. In (a), arrows point to the exposed lipid bilayer. (b) Magnified image of the square area in (a). (c) The cross section analysis along the line in (b). (d) The same area in (a) after treatment by M $\beta$ CD, in which arrows indicate the lipid raft domains. (e) Height distribution of particles in the membrane after Proteinase K digestion. Scale bars: 5  $\mu$ m in (a) and (d), 200 nm in (b).

Methyl- $\beta$ -cyclodextrin (M $\beta$ CD) is the most widely used reagent to extract cholesterol from plasma membranes and accordingly disrupt lipid rafts<sup>22, 28</sup>. In order to observe the interaction between M $\beta$ CD and erythrocyte membranes after Proteinase K digestion, M $\beta$ CD was injected into the AFM sample chamber, and successive real-time AFM images in the same area were recorded to monitor the changes occurred in situ. As shown in Fig.3d, after most of the membrane proteins were digested by Proteinase K, the inner leaflet membranes were eroded quickly by M $\beta$ CD. The resulting branched membranes exhibit great similarity with that of human erythrocyte membranes similarly treated by Proteinase K and M $\beta$ CD. The eroded domains, pointed by arrows, represent the irregular lipid raft domains in the erythrocyte membranes. Most of those undigested proteins by Proteinase K still stand above the lipid bilayer, indicating that they are non-raft associated proteins. To our knowledge, for the first time, we verified the existence of lipid rafts in chicken erythrocyte membranes by in situ observing the erosion of lipid rafts by M $\beta$ CD.

### Detecting the exposed amino groups in the inner and outer leaflets of erythrocyte membranes by force spectroscopy

AFM based single molecule force spectroscopy has developed as a powerful tool for sensing the forces and examining the dynamic processes between conjugated biological pairs at the single molecule level<sup>29, 30</sup>. It could detect the intra- and intermolecular force down to piconewton<sup>31</sup>. To confirm the location of proteins in the inner and outer leaflet of erythrocyte membranes, we functionalized the AFM tips with glutaraldehyde which binds the exposed amino groups of membrane proteins and engaged the force measurement on both sides of erythrocyte membranes.

Thousands of force curves were recorded at various positions on both sides of chicken erythrocyte membranes. A typical force curve acquired in the inner leaflet of erythrocyte membranes is shown in Fig.4a. There are multiple force peaks when withdrawing the AFM tip from the membrane surface, indicating a large number of exposed amino groups in the inner leaflet of erythrocyte membranes. As shown in Fig.4b, there is no force event when engaging force measurement on the outer leaflet of erythrocyte membranes, which demonstrates no exposed amino groups in the outer leaflet of erythrocyte membranes. The loading rate is 4.0 nN/s during force spectroscopy measurements. The binding probability (the force curves with the specific unbinding events divided by the overall force curves) is 86.4%

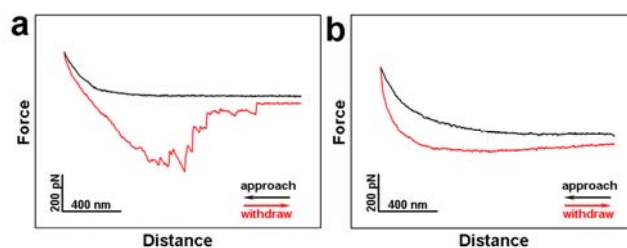


Fig. 4 The typical force-distance curves acquired on the inner (a) and outer (b) leaflet of chicken erythrocyte membranes by glutaraldehyde-functionalized AFM tip. In (a), the force curve shows multiple force peaks, while no force peak was observed in (b).

(15000 in total) and 3.8% (11000 in total) in the inner and outer leaflet of erythrocyte membranes, respectively. This result further demonstrates that the inner leaflet of erythrocyte membranes is crowded by dense proteins whereas the outer leaflet of erythrocyte membranes is devoid of exposed proteins. Probably, the membrane proteins in the outer membrane side are covered by the oligosaccharides but not protruding out of cell membranes with exposed amino group<sup>25, 26</sup>.

## Conclusions

In this study, we directly observed erythrocytes and erythrocyte membranes from chicken by AFM at molecular resolution under quasi-native conditions. In morphology, chicken erythrocytes are oval, biconvex discs with elliptical nucleus protruding in the central region, which is similar with Crucian carp erythrocytes except smaller in size. The size of erythrocyte decreases from Crucian carp to chicken, human (Table 1), corresponding well with erythrocyte evolutionary law which discloses a decrease in erythrocyte size during the evolution from lower vertebrate to birds, mammals. The height of chicken erythrocyte membranes is  $16.5 \pm 3.6$  nm, slightly thinner than that of Crucian carp erythrocyte but thicker than that of human erythrocyte. Considering that the measured thickness of lipid bilayer is roughly the same among these species, the different size or arrangement of protein particles above the membranes may contribute to the larger membrane thickness and roughness. The thickness of erythrocyte membranes is proportional to erythrocyte size, which might play an important role in erythrocyte osmotic fragility with more thicker cell membrane guaranteeing stronger osmotic resistance and longer erythrocyte life span from mammalian to birds, lower vertebrate<sup>32</sup>.

**Table 1** Comparison of parameters of chicken, fish and human erythrocyte membranes.

	$S_m$ ( $\mu\text{m}$ )	$T_m$ (nm)	$R_m$ (nm)		$P_a$ (%)		$T_l$ (nm)
			Inner	Outer	Inner	outer	
Fish <sup>a</sup>	$(23.7 \pm 3.1) \times (15.2 \pm 3.3)$	$18.2 \pm 3.0$	$3.1 \pm 0.7$	$0.56 \pm 0.06$	98.5	6.5	$3.5 \pm 0.6$
Chicken	$(14.2 \pm 3.0) \times (8.9 \pm 1.6)$	$16.5 \pm 3.6$	$3.4 \pm 0.8$	$0.47 \pm 0.05$	86.4	3.8	$3.1 \pm 0.7$
Human <sup>b</sup>	8	10	1.9	0.18	-	-	$2.9 \pm 0.4$

$S_m$ , size of the membrane;  $T_m$ , thickness of the membrane;  $R_m$ , the average roughness of the membrane;  $P_a$ , percentage of exposed amino groups in the membrane;  $T_l$ , thickness of the lipid bilayer; a, data from reference 9; b, data from reference 8.

High resolution image by AFM on both sides of chicken erythrocyte membranes revealed that the outer leaflet of erythrocyte membranes is quite smooth without proteins protruding out of cell surface, whereas the inner leaflet of erythrocyte membranes is very rough with dense proteins standing closely to each other above the lipid bilayer. This asymmetry is further confirmed by single-molecule force spectroscopy, which indicates the amino groups are exposed in the inner leaflet membrane but inaccessible by the AFM tip in the outer leaflet membrane. In situ, real time AFM visualize the

erosion of lipid raft by M $\beta$ CD in Proteinase K treated inner membrane leaflet, which provides the first direct evidence of existence of lipid rafts in chicken erythrocyte membranes. The asymmetric distribution of proteins on both sides of chicken erythrocyte membranes fits well with the semi-mosaic model of human and fish erythrocyte membrane structure, which highlights the smooth outer membrane leaflet and the protein covered inner membrane leaflet<sup>8, 9</sup>. This study of chicken erythrocyte membranes provides consistency of membrane structure in mammalian, birds and lower vertebrate erythrocytes and extends the semi-mosaic model of erythrocytes membrane structure from mammalian, lower vertebrate to birds. This similarity of membrane structure between mammalian, birds and lower vertebrate erythrocytes further lead us to believe that the asymmetry of membrane structure exists universally in all living cells.

## Acknowledgements

This work was supported by Ministry of Science and Technology of China (MOST, 2011CB933600), National Natural Science Foundation of China (NSFC, 21373200, 31330082, 21203177).

## Notes and references

<sup>a</sup>University of Chinese Academy of Sciences, Beijing 100049, P.R. China.  
<sup>b</sup>State Key Laboratory of Electroanalytical Chemistry, Changchun Institute of Applied Chemistry, Chinese Academy of Sciences, Changchun, Jilin 130022, P.R. China.

E-mail address: hdwang@ciac.ac.cn; Tel: +86-431-85262453; fax: +86-431-85262864.

†Electronic Supplementary Information (ESI) available: [Experimental procedures of the isolation, preparation of chicken erythrocyte for AFM imaging; Protocols of functionalization of the AFM tips for force spectroscopy]. See DOI: 10.1039/c000000x/

1. K. Keren, *Eur. Biophys. J.*, 2011, **40**, 1013-1027.
2. D. J. Muller, *Biochemistry*, 2008, **47**, 7986-7998.
3. D. Fotiadis, *Curr. Opin. Biotech.*, 2012, **23**, 510-515.
4. J. J. Heinisch, P. N. Lipke, A. Beaussart, S. E. K. Chatel, V. Dupres, D. Alsteens and Y. F. Dufrene, *J. Cell Sci.*, 2012, **125**, 4189-4195.
5. S. J. Singer and G. L. Nicolson, *Science*, 1972, **175**, 720-731.
6. K. Simons and E. Ikonen, *Nature*, 1997, **387**, 569-572.
7. G. Vereb, J. Szollosi, J. Matko, P. Nagy, T. Farkas, L. Vigh, L. Matyus, T. A. Waldmann and S. Damjanovich, *Proc. Natl. Acad. Sci. USA*, 2003, **100**, 8053-8058.
8. H. D. Wang, X. Hao, Y. P. Shan, J. G. Jiang, M. J. Cai and X. Shang, *Ultramicroscopy*, 2010, **110**, 305-312.
9. Y. Tian, M. Cai, W. Zhao, S. Wang, Q. Qin, and H. Wang, *Chin. Sci. Bull.*, 2014, **59**, 2582-2587.
10. V. B. Kaiser, M. van Tuinen and H. Ellegren, *Mol. Biol. Evol.*, 2007, **24**, 338-347.
11. K. Bhattacharyya, T. Guha, R. Bhar, V. Ganesan, M. Khan and R. L. Brahmachary, *Anat. Rec.*, 2004, **279**, 671-675.
12. J. A. Claver and A. I. E. Quaglia, *J. Exot. Pet Med.*, 2009, **18**, 87-97.
13. H. Hagerstrand, M. Danieluk, M. Bobrowska-Hagerstrand, T. Holmstrom, V. Kralj-Iglic, C. Lindqvist and M. Nikinmaa, *Mol.*

## Journal Name

- 1  
2  
3  
4  
5  
6  
7  
8  
9  
10  
11  
12  
13  
14  
15  
16  
17  
18  
19  
20  
21  
22  
23  
24  
25  
26  
27  
28  
29  
30  
31  
32  
33  
34  
35  
36  
37  
38  
39  
40  
41  
42  
43  
44  
45  
46  
47  
48  
49  
50  
51  
52  
53  
54  
55  
56  
57  
58  
59  
60
- Membr. Biol.*, 1999, **16**, 195-204.
14. A. M. Ferlazzo, G. Bruschetta, P. Di Pietro, P. Medica, A. Notti and E. Rotondo, *Vet. Res. Commun.*, 2011, **35**, 521-530.
15. C. Drew, V. Ball, H. Robinson, J. C. Ellory and J. S. Gibson, *Bioelectrochemistry*, 2004, **62**, 153-158.
16. L. Picas, F. Rico, M. Deforet and S. Scheuring, *Acs Nano*, 2013, **7**, 1054-1063.
17. I. Medalsy, U. Hensen and D. J. Muller, *Angew. Chem. In. Ed.*, 2011, **50**, 12103-12108.
18. Y. Tian, J. Li, M. Cai, W. Zhao, H. Xu, Y. Liu and H. Wang, *RSC Adv.*, 2013, **3**, 708-712.
19. H. Xu, W. Su, M. Cai, J. Jiang, X. Zeng and H. Wang, *Plos One*, 2013, **8**, e61596.
20. Y. Suzuki, N. Sakai, A. Yoshida, Y. Uekusa, A. Yagi, Y. Imaoka, S. Ito, K. Karaki and K. Takeyasu, *Sci. Rep.*, 2013, **3**, 2131.
21. T. Uchihashi, R. Iino, T. Ando and H. Noji, *Science*, 2011, **333**, 755-758.
22. J. C. Lawrence, D. E. Saslowsky, J. M. Edwardson and R. M. Henderson, *Biophys. J.*, 2003, **84**, 1827-1832.
23. M. Cai, W. Zhao, X. Shang, J. Jiang, H. Ji, Z. Tang and H. Wang, *Small*, 2012, **8**, 1243-1250.
24. E. Nagao, T. Arie, D. W. Dorward, R. M. Fairhurst and J. A. Dvorak, *J. Struct. Biol.*, 2008, **162**, 460-467.
25. M. Duk, H. Krotkiewski, T. V. Stasyk, M. Lutsik-Kordovsky, D. Syper and E. Lisowska, *Arch. Biochem. Biophys.*, 2000, **375**, 111-118.
26. M. J. Weise and V. M. Ingram, *J. Biol. Chem.*, 1976, **251**, 6667-6673.
27. H. N. Allen MJ, Balooch M, Tench RJ, Siekhaus WJ, Balhorn R, *Ultramicroscopy*, 1992, **42-44**, 1095-1100.
28. M. Hao, S. Mukherjee and F. R. Maxfield, *Proc. Natl. Acad. Sci. USA* 2001, **98**, 13072-13077.
29. M. Zhang, S. Wu, W. Zhou and B. Xu, *J. physic. chem. B*, 2012, **116**, 9949-9956.
30. P. Hinterdorfer, W. Baumgartner, H. J. Gruber, K. Schilcher and H. Schindler, *Proc. Natl. Acad. Sci. USA*, 1996, **93**, 3477-3481.
31. W. Zhao, M. Cai, H. Xu, J. Jiang and H. Wang, *Nanoscale*, 2013, **5**, 3226-3229.
32. K. J. Aldrich, D. K. Saunders, L. M. Sievert and G. Sievert, *Transac. KS Acad. Sci.*, 2006, **109**, 149-158.